Endogenous tenascin-C enhances glioblastoma invasion with reactive change of surrounding brain tissue

Eishu Hirata,[1,2] Yoshiki Arakawa,[1,5] Mitsuaki Shirahata,[1] Makoto Yamaguchi,[1] Yo Kishi,[1] Takashi Okada,[1] Jun A. Takahashi,[3] Michiyuki Matsuda[2] and Nobuo Hashimoto[4]

[1]Department of Neurosurgery, [2]Department of Pathology and Biology of Diseases, Kyoto University Graduate School of Medicine, Kyoto 606-8507; [3]Department of Neurosurgery, Kitano Hospital, Osaka 530-8480; [4]National Cardiovascular Center, Osaka 565-8565, Japan

(Received November 25, 2008/Revised March 27, 2009/Accepted April 6, 2009/Online publication May 13, 2009)

Tenascin-C is an extracellular matrix glycoprotein implicated in embryogenesis, wound healing and tumor progression. We previously revealed that tenascin-C expression is correlated with the prognosis of patients with glioblastoma. However, the exact role of endogenous tenascin-C in regulation of glioblastoma proliferation and invasion remains to be established. We show here that endogenous tenascin-C facilitates glioblastoma invasion, followed by reactive change of the surrounding brain tissue. Although shRNA-mediated knockdown of endogenous tenascin-C does not affect proliferation of glioblastoma cells, it abolishes cell migration on a two-dimensional substrate and tumor invasion with brain tissue changes in a xenograft model. The tyrosine phosphorylation of focal adhesion kinase, a cytoplasmic tyrosine kinase that associates with integrins, was decreased in tenascin-C-knockdown cells. In the analysis of clinical samples, tenascin-C expression correlates with the volume of peritumoral reactive change detected by magnetic resonance imaging. Interestingly, glioblastoma cells with high tenascin-C expression infiltrate brain tissue in an autocrine manner. Our results suggest that endogenous tenascin-C contributes the invasive nature of glioblastoma and the compositional change of brain tissue, which renders tenascin-C as a prime candidate for anti-invasion therapy for glioblastoma. (*Cancer Sci* 2009; 100: 1451–1459)

Glioblastoma is the most common and most agressive primary brain tumor in adults. As it is recalcitrant to any current treatment including surgery, radiotherapy and chemotherapy, the median survival time is less than 1 year.[1] Glioblastoma is characterized by extensive invasiveness into the surrounding brain tissue, which makes it impossible to provide a cure by surgical resection.[2] For these reasons, recurrent tumors develop adjacent to the resection cavity and in the contralateral hemisphere. Magnetic resonance (MR) imaging is the standard clinical examination for the diagnosis of glioblastoma. Glioblastoma is a radiologically heterogeneous tumor with severe edema of the brain parenchyma. Gadolinium enhancement often demonstrates 'ring enhancement', which represents central necrosis and enhancing rim of glioblastoma cells, with accompanying microvascular hyperplasia and increased permeability.[3] The fluid-attenuated inversion recovery (FLAIR) sequence yields heavily T2-weighted MR images of the brain with suppression of the cerebrospinal fluid signal. Glioblastoma induces vasogenic edema and changes the composition of brain parenchyma. As a possible mechanism, glioblastoma-derived factors downregulate endothelial tight junction proteins, resulting in impairment of the blood–brain barrier.[4] Various extracellular matrices, such as matrix metalloproteinase (MMP), collagen type IV and laminin are increased.[5] For these reasons, FLAIR images can detect the peritumoral change in brain tissue as hyperintense.[6]

This invasive capacity of glioma cells is driven by complex molecular processes involving the remodeling of extracellular matrix (ECM), intracellular signaling and cytoskeletal reorganization.[7] Several genes involved in glioma invasiveness have been identified, including those coding for chemoattractants, signaling molecules, adhesion molecules and MMP.[8–10] Migration of glioma cells involves active intracellular signaling with molecules such as PI3 K, focal adhesion kinase (FAK) and small GTPase proteins.[11] For example, the Rho GTPase RhoA and its effector, mDia1, regulate cell polarity and focal adhesion turnover in migrating glioma cells by localizing adenomatous polyposis coli (Apc) and proto-oncogene-encoded c-Src tyrosine kinase (c-Src).[12] Src binding to FAK contributes to src activation, promoting further phosphorylation of FAK at additional tyrosines, which is responsible for efficient disassembly of focal adhesion.[13] Meanwhile, glioma invasion requires the detachment of the cell from the ECMs and/or the adjacent cells as well as proteolytic degradation of ECMs around the tumor.[2]

Tenascin-C, a component of the ECMs, is highly expressed in many malignancies, including glioblastoma.[14–17] Many previous reports have provided important insights into the biological function of tenascin-C. However, the mechanisms by which it signals are not yet clear, and these appear to be variable across cell types and experimental models.[14] In addition, most studies have relied upon exogenous tenascin-C and *in vitro* models,[18–22] while few have focused upon this protein *in vivo*. Curiously, melanoma invasion *in vivo* was only slightly promoted in knockout mice lacking tenascin-C.[23]

In this study, therefore, we investigated the role of endogenous tenascin-C in glioblastoma invasion and proliferation by using shRNA-mediated knockdown of its expression. To characterize the function of intrinsic tenascin-C of glioblastoma cells *in vivo*, we used a glioblastoma xenograft model. In the analysis of resected tumor in patients with glioblastoma, we examined the correlation between tenascin-C expression, glioblastoma invasion and secondary tissue change of brain parenchyma. Our results provide a new insight into the role of endogenous tenascin-C in glioblastoma progression.

Materials and Methods

Antibodies and reagents. The following primary and secondary antibodies were used for Western blot analysis, immunocytochemistry or immunohistochemistry: anti-human tenascin-C mouse monoclonal antibody (Abcam, Cambridge, MA), anti-human/

[5]To whom correspondence should be addressed.
E-mail: yarakawa@sb3.so-net.ne.jp

doi: 10.1111/j.1349-7006.2009.01189.x

mouse tenascin-C rat monoclonal antibody (R&D Systems, Inc., Minneapolis, MN); anti-human tenascin-C mouse monoclonal antibody (clone 49; Novocastra Laboratories, Newcastle, UK); anti-human Ki-67 mouse monoclonal antibody (clone MM1, Novocastra Laboratories); anti-human α-tubulin mouse monoclonal antibody (TU-02; Santa Cruz Biotechnology, Santa Cruz, CA); anti-phosphotyrosine mouse monoclonal antibody (4G10) (Millipore Corporate Headquarters, Billerica, MA); anti-phosphotyrosine mouse monoclonal (P-Tyr-100) anti-phospho-p130 CAS (Tyr165) rabbit polyclonal antibodies (Cell Signaling Technology, Beverly, MA); anti-p130 CAS, anti-FAK (clone 77) and anti-phospho-FAK (pY397) mouse monoclonal antibodies (BD Bioscience, San Jose, CA); and AlexaFluora 405-goat anti-mouse and 546-goat anti-rat IgG antibodies (Invitrogen, Carlsbad, CA). Rhodamine-conjugated phalloidin (Invitrogen) was used to stain F-actin.

Cell culture. LN229 human glioblastoma cells were obtained from the American Type Culture Collection (Manassas, VA) and maintained in Dulbecco's modified Eagle's medium (DMEM) containing 10% fetal bovine serum (FBS) at 37°C in a humidified atmosphere containing 5% CO_2. For the evaluation of cell growth, 5×10^4 glioma cells were seeded onto 24-well plates, and the number of viable cells was counted on days 2 and 4.

Lentiviral shRNA-mediated RNA interference. The knockdown vector was constructed by using a shRNA expression lentiviral vector. Lentiviral production and infection were described previously.[24] The target sequence for RNA interference was selected from human tenascin-C candidate sequences that are available from GenomeWide siRNA (Qiagen, Hilden, Germany). The selected target sequence for tenascin-C corresponded to the mRNA of the coding region, nt 3853–3871, 5′-GCTGGGAT GCCCTCAAACT-3′. The sequence 5′-GATTCTCCGAACG TGTCAC-3′ was used as a negative control.

Fluorescence microscopy and image analysis. Our method of fluorescence microscopy is described previously.[25] Glioma cells were cultured on non-coated and fibronectin-coated glass-bottom dishes in DMEM with 10% FBS at 37°C in a humidified atmosphere containing 5% CO_2. After 24 h, cells were fixed with 4% paraformaldehyde, permeabilized with 0.2% Triton X-100 in PBS, blocked with 5% BSA and 1% FBS in PBS, and incubated with the primary antibody overnight, followed by incubation with fluorophore-conjugated secondary antibodies. After rinsing in PBS, the cells were imaged with a confocal laser scanning microscope (FV1000; Olympus, Tokyo, Japan). To compare the level of tyrosine phosphorylation at the focal adhesion, the area and intensity of the phospho-tyrosine signal at focal adhesions were measured and corrected by MetMorph software (Molecular Devices, Sunnyvale, CA). The analyses were in the control (3980 focal adhesions in 30 cells) and the tenascin-C knockdown (5072 focal adhesions in 36 cells).

Western blot analysis. Cultured cells at 80% confluency were washed with PBS and the cellular proteins were extracted in cell lysis buffer (Invitrogen) supplemented with 2.5% 2-mercaptoethanol and boiled at 95°C for 5 min. Equal amounts of proteins were electrophoresed in 4–12% precasted Tris-Bis gels (Invitrogen) and transferred onto nitrocellulose membranes with the use of the Iblot system (Invitrogen). After blocking with 5% bovine serum albumin (BSA) in Tris-buffered saline (TBS) with 0.05% Tween 20 (TBS–T), the membrane was incubated with primary antibody overnight at 4°C, followed by washing in TBS–T and incubation with a horseradish peroxidase-conjugated goat anti-mouse IgG diluted in TBS–T with 5% skim milk for 1 h at room temperature. The labeled proteins were visualized with ECL plus Western blot detection system (GE Healthcare, Piscataway, NJ).

Monolayer wound healing assay and cell locomotion assay. A wound was made by scratching the monolayer cells with a pipette tip.[12] After the removal of scratched cells, the cells were cultured for 14 h. Photographs of cells were taken before and after wounding to measure the width of the wound. For the analysis of single cell locomotion, cells were seeded onto either a non-coated or tenascin-C coated (10 μg/mL) glass-bottom dish 24 h before imaging. Cells were imaged every 5 min for 12 h with an Olympus IX81 inverted microscope (Olympus) equipped with the ZDC autofocusing system. Cell track and velocity were calculated with MetMorph software.

Mouse xenograft glioma model. Animal care and experiments complied with Japanese community standards on the care and use of laboratory animals. For intracranial transplantation, glioma cells (5×10^5 cells/5 μL of PBS) were stereotactically transplanted into the right striatum of 9-week-old-male nude mice (BALB/cAJc1-nu) as described elsewhere.[26] Neurological defects and emaciation of the mice were carefully observed every day. Three weeks after transplantation, the brain specimens were prepared after euthanasia. The brain tissues were fixed in 4% paraformaldehyde in PBS. Sectioned coronally at the point of cellular implantation, the brain tissue was embedded into Optimal Cutting Temprature (O.C.T.) compound (Sakura, Tokyo, Japan) and frozen in liquid nitrogen. Twenty-micrometer sections were cut and mounted on silane-coated slides, and observed through a fluorescence microscope system (BX51N-34-FL-1; Olympus).

Resected glioblastoma samples, quantitative reverse transcription PCR (RT-PCR) and immunohistochemistry. Histological diagnosis was conducted according to the WHO Classification of Brain Tumors.[1] Tumor specimens for molecular research were snap-frozen immediately after surgical resection and kept at –80°C. For the sampling of tumor tissues corresponding to the gadolinium-enhanced lesion or hyperintense area of FLAIR sequences, we used either StealthStation TRIA plus with Cranial v4.0 software (Medtronic Sofamor-Danek), or Vector Vision Compact Navigation System with VV Cranial v7.5 software (BrainLab AG, Heim Stetten, Germany). The study protocol was approved by the institutional review board of Kyoto University, and written informed consent was obtained from each patient. For the immunohistochemical analysis in resected glioblastoma samples, the conventional avidin–biotin–peroxidase complex method was used as described elsewhere.[27] For quantitative reverse RT-PCR, we used methods described previously.[28] The second-derivative maximum method was used for crossing-point determination using LightCycler Software 3.3 (Roche, Basel, Switzerland). GAPDH was used as an internal control. The following primer sets were used: forward, 5′-GTCACCGTGTCAACCTGATG-3′, and reverse, 5′-GCCTGCCTTCAAGATTTCTG-3′, for tenascin-C; forward, 5′-TGACAACAGCCTCAAGATCA-3′, and reverse, 5′-CTGTGGTCATGAGTCCTTCC-3′, for GAPDH. The conditions for PCR were 45 cycles of 95°C for 10 s for denaturation, 56°C for 5 s for annealing and 72°C for 10 s for extension.

Measurement of tumor volume and definition of 'FLAIR/Enhanced volume ratio'. To calculate 'FLAIR/Enhanced volume ratio' in each patient, we defined two tumor volumes on the multislice MR images. For measurement of 'Enhanced tumor volume', the border of the tumor area was determined at the enhancing rim on the T1-weighted images with gadolinium enhancement. For measurement of 'FLAIR hyperintensity volume', the border of the tumor area was determined at the outer rim of the hyperintensity area in FLAIR sequences. The planar dimension was analyzed using NIH Image software. In either case, tumor volumes were calculated by the formula: Σ([planar dimension] × [slice distance]). 'FLAIR/Enhanced volume ratio' was defined by the formula: ([FLAIR tumor volume] – [gadolinium-enhanced tumor volume])/[gadolinium-enhanced tumor volume]) (%).

Statistical analysis. The Spearman rank correlation test was used to analyze correlations between tenascin-C expression and Invasion Index. When two groups were compared, an unpaired Student's *t*-test was applied.

doi: 10.1111/j.1349-7006.2009.01189.x

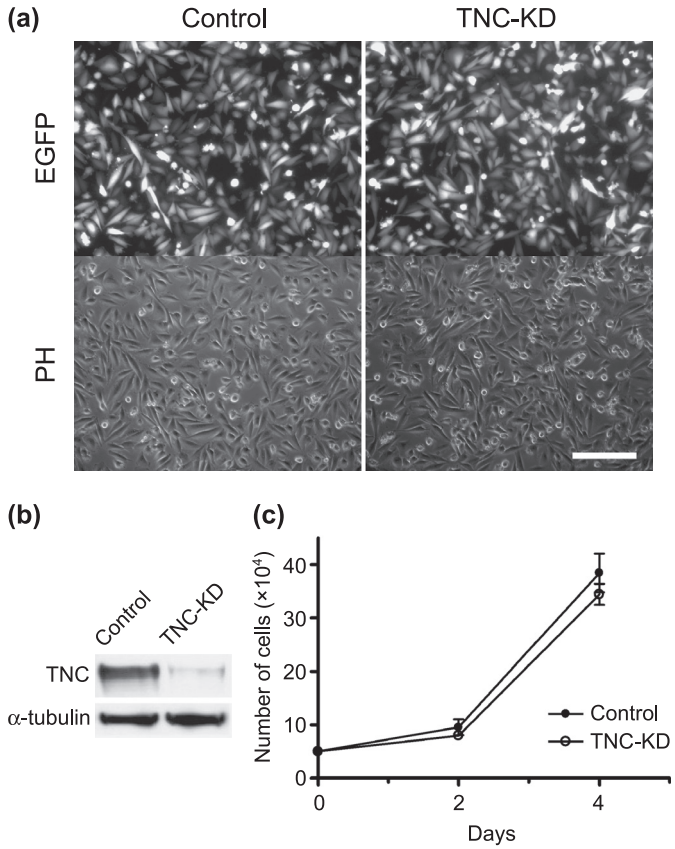

Fig. 1. shRNA-mediated knockdown of tenascin-C does not affect cell proliferation in LN229 glioblastoma cells. (a) Lentiviral shRNA against control and tenascin-C was introduced into LN229 cells and IRES-mediated EGFP expressions were seen as an infection marker. Fluorescence (EGFP) and phase-contrast (PH) images are shown. (b) Representative immunoblot of tenascin-C and α-tubulin in shRNA-mediated protein knockdown against control and tenascin-C in LN229 cells. (c) Quantification of cell growth in control and tenascin-C knockdown cells 2 and 4 days after cell plating. Data are shown as mean ± SD (n = 3). Scale bar, 200 μm; TNC-KD, tenascin-C-knockdown cells.

Results

shRNA-mediated knockdown of endogenous tenascin-C does not affect glioblastoma cell proliferation. The biological functions of tenascin-C have been implicated in tumor progression.[29] However, relevant studies to date have been performed using exogenous tenascin-C. To examine the role of endogenous tenascin-C in glioblastoma cells, LN229 cells were transduced with a lentiviral shRNA sequence against tenascin-C to knock down this protein's expression. The lentiviral transduction efficiencies of tenascin-C shRNA and control shRNA were consistently greater than 90% as measured by IRES-mediated enchanced-green fluorescent protein (EGFP) expression (Fig. 1a). Tenascin-C is highly expressed in LN229 cells, and the shRNA for tenascin-C significantly reduced its protein expression (Fig. 1b). Although tenascin-C has been shown to mediate its effects on cell proliferation via mitogen-activated protein kinase signaling in cells plated on fibronectin,[20] there was no significant difference in the growth rates between the control shRNA and the tenascin-C-knockdown glioblastoma cells on the substrata without fibronectin (Fig. 1c). This observation indicates that endogenous tenascin-C does not accelerate cell growth.

Endogenous tenascin-C regulates cell motility in LN229 glioblastoma cells. Addition of extrinsic tenascin-C promotes glioma cell migration and invasion.[18] We tested whether endogenous tenascin-C expression is similarly involved in glioma cell motility, and found that tenascin-C knockdown inhibited glioma cell migration in the monolayer wound healing assay (Fig. 2a,b). Cell migration requires remodeling of the actin cytoskeleton and assembly and disassembly of focal adhesions.[12] For this reason, we hypothesized that endogenous tenascin-C knockdown alters cell adhesion, resulting in diminished cell motility. We examined the cytoskeletons induced by endogenous tenascin-C knockdown. On the fibronectin, the formation of focal adhesion is decreased in the control cells, but it was not clearly changed in tenascin-C-knockdown cells, which is consistent with that of past studies. Interestingly, tyrosine phosphorylation of focal adhesion is decreased in tenascin-C-knockdown cells on non-coated coverslips (Fig. 2c–e). It has been reported that tenascin-C suppresses RhoA activity and inhibits the formation of actin stress fibers.[30] Therefore, we examined the involvement of RhoA in this effect on cell migration; however, no apparent difference was detected in GTP-RhoA (active form of RhoA) (data not shown). In focal adhesions, FAK and p130 Cas (Crk-associated substrate) colocalize with integrins.[13] We found that tyrosine phosphorylation of FAK, but not p130 Cas, was decreased in tenascin-C-knockdown cells. When we analyzed the LN229 cell locomotion by cell-tracking analysis, tenascin-C knockdown glioma cells significantly decreased the mean velocity and the distance from the origin. Another question was whether or not cytoplasmic tenascin-C can act directly on cell motility. Strikingly, coating the tissue culture dishes with tenascin-C restored the migration velocity of the tenascin-C knockdown cells to the level of the parent cells (Fig. 3), which indicates that tenascin-C regulates glioblastoma cell migration in an autocrine manner.

Tenascin-C-knockdown decreases glioblastoma cell invasiveness and reactive change of peritumoral brain tissue. We next examined whether endogenous tenascin-C is involved in glioblastoma cell invasion *in vivo*. We used a xenograft model implanting control and tenascin-C-knockdown LN229 cells into the striatum of BALB/c nude mice. Using this model, we evaluated the invasiveness of glioblastoma cells 3 weeks after implantation. Control shRNA cells exhibited tumor growth and infiltration into the surrounding brain tissue, forming small tumor clusters distinct from the tumor core (Fig. 4a,c). Histopathologically, edematous change was observed in the brain parenchyma containing glioblastoma infiltration (Fig. 4b). Intercellular tenascin-C was also diffusely deposited not only in the tumor core but also in the surrounding brain tissue with glioblastoma cell infiltration (Fig. 4d). In contrast, although tumor size of tenascin-C-knockdown LN229 cell was approximately equal to that of control cells (Fig. 4i), the number of infiltrating glioma cells and tumor clusters in the surrounding brain were decreased (Fig. 4g). As expected, these cells deposited significantly less tenascin-C than the control (Fig. 4h), and the edematous change was decreased in the brain parenchyma around the tumor (Fig. 4f). The infiltrating control cells show dense cytoplasmic tenascin-C (Fig. 4c,d, white rectangles). Quantification of tumor cluster number revealed that tenascin-C knockdown decreased cluster formation by approximately half, compared with control cells (Fig. 4j). These results indicate that endogenous tenascin-C promotes glioblastoma cell invasion and the adjacent reactive change of the brain parenchyma but is not involved in tumor growth in the glioblastoma xenograft models.

Tenascin-C expression correlates with the volume of the reactive brain tissue in glioblastoma. Our experimental study showed that endogenous tenascin-C promotes glioblastoma invasion and a secondary reactive change of the peritumoral tissue. The reactive change of brain tissue contains vasogenic edema and compositional change of brain tissue induced by tumor cell infiltration. In modern MR imaging, the tumor core is enhanced by gadolinium and the peritumoral change in brain parenchyma is seen as a

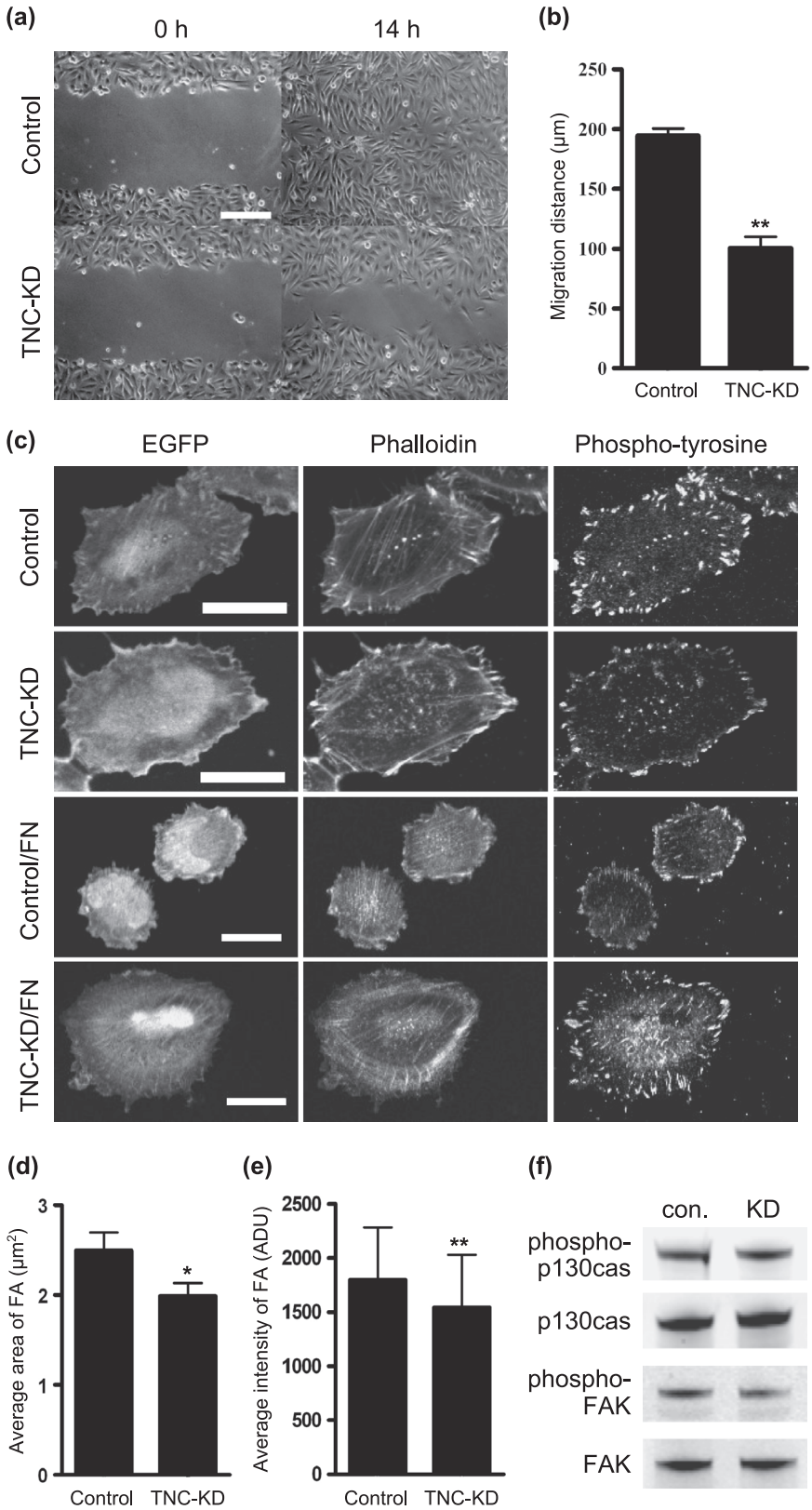

Fig. 2. Endogenous tenascin-C regulates cell motility in LN229 glioblastoma cells. (a) The confluent monolayers of the control and tenascin-C-knockdown LN229 cells were photographed 0 and 14 h after scraping. (b) The distance of cell-edge movements 14 h after scraping is shown as mean ± SD ($n = 3$). (c) F-actin (phalloidin) and tyrosine-phosphorylated proteins were stained in the control and tenascin-C-knockdown cells on the non-coated and fibronectin coated coverslips. (d,e) The average area and intensity of tyrosine-phosphorylation signals in the control and tenascin-C knockdown cells stained by phosphor-tyrosine antibody on the non-coated glass-bottom dishes are measured and shown as mean ± SE (control, $n = 30$; TNC-KD, $n = 36$). (f) Representative immunoblot of phosphorylated p130Cas and FAK in shRNA-mediated protein knockdown against control and tenascin-C in LN229 cells. TNC-KD, tenascin-C-knockdown cells; **, $P < 0.001$; scale bar, 200 μm.

hyperintense region by FLAIR sequences (Fig. 5a). It is therefore possible that the peritumoral hyperintensity area represents the secondary change induced by tenascin-C-facilitated glioblastoma cell invasion. We examined the correlation between the FLAIR/Enhanced volume (F/E) ratio (indicating the volume of peritumoral tissue change), with tenascin-C mRNA expression in resected tumors from 16 glioblastoma patients. Strikingly, tenascin-C expression significantly correlates with

doi: 10.1111/j.1349-7006.2009.01189.x

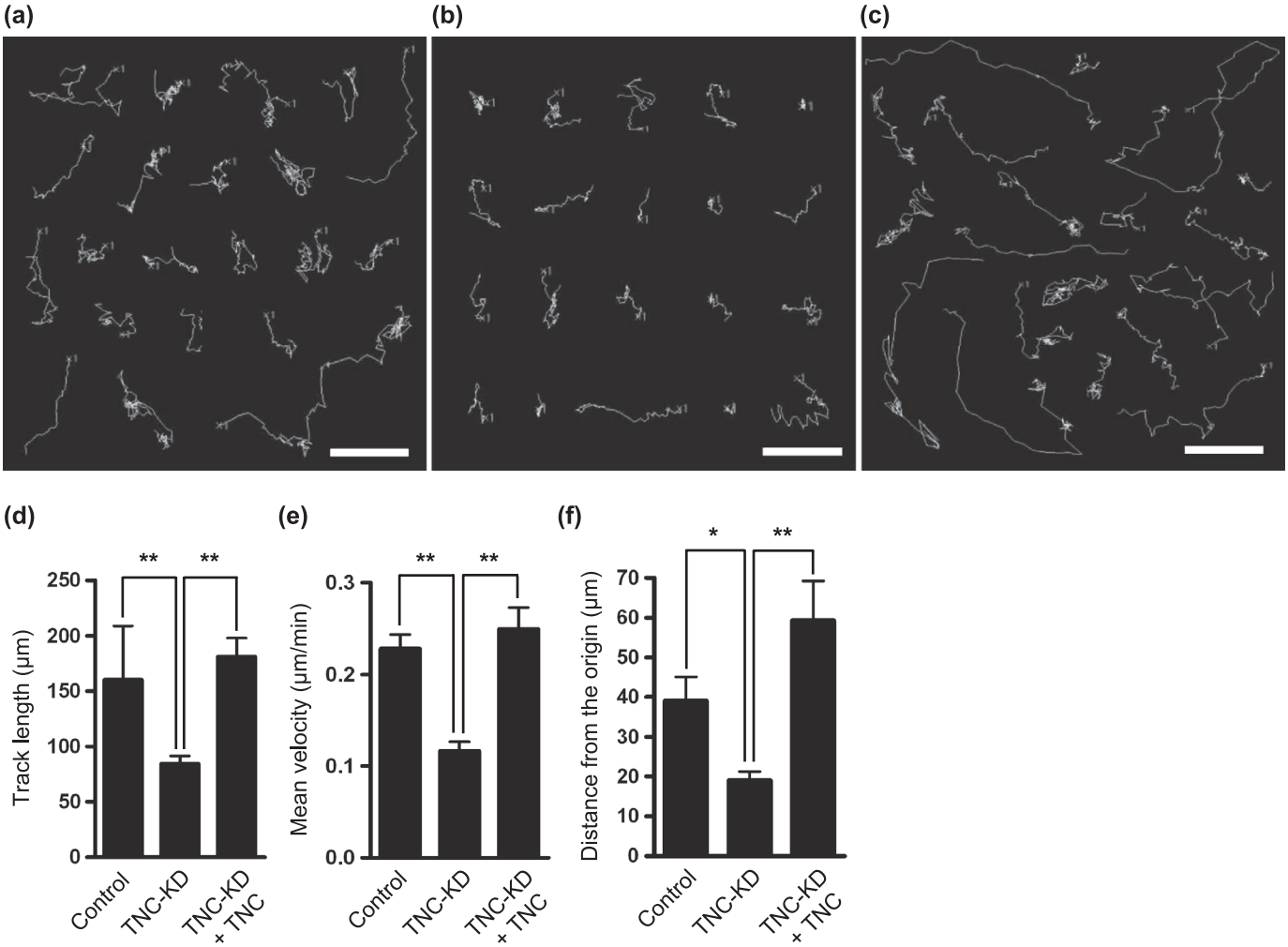

Fig. 3. Endogenous tenascin-C activates glioblastoma cell locomotion. Cell tracking of (a) control cells, (b) tenascin-C-knockdown cells and (c) tenascin-C-knockdown with addition of exogenous tenascin-C. Cells were imaged every 5 min for 12 h under microscopy. (d) Track length (μm). (e) Mean velocity (μm/min). (f) Distance from the origin. Tracks and velocities were calculated with MetMorph software (Molecular Devices, Sunnyvale, CA). TNC-KD, tenascin-C-knockdown cells; TNC-KD + TNC, tenascin-C-knockdown cells with exogenous tenascin-C; *, $P < 0.01$; **, $P < 0.001$; scale bars, 50 μm.

the volume of the peritumoral tissue change (Spearman correlation test, $P = 0.005$, $r = 0.77$) (Fig. 5b), although it does not correlate with the proliferation index by a mitotic marker Ki-67 staining (Spearman correlation test, $P = 0.272$, $r = –0.29$) (Fig. 5c).

The localization of tenascin-C in resected glioblastomas has been described in the perivascular and intercellular spaces. However, it is unclear to what extent tenascin-C is expressed around the tumor.[31] We therefore examined the localization of tenascin-C in resected glioblastoma sections obtained from either the tumor core (gadolinium-enhanced area) or the surrounding lesion (hyperintensity area of FLAIR imaging) by using intraoperative navigation systems. In patients with high and low F/E ratios, intercellular deposition of tenascin-C was detected in the tumor core (Fig. 6a,b, upper panels, TNC). The peritumoral brain parenchyma, showing hyperintensity with FLAIR imaging, contained glioblastoma cells undergoing mitosis (Fig. 6a,b, lower panels, Ki-67). In the patient with a high F/E ratio, a number of glioblastoma cells infiltrated in the peritumoral brain tissue and exhibited high deposition of tenascin-C in their cytoplasm (Fig. 6b, lower panels). Based on these results, one possible mechanism of glioblastoma progression is that glioblastoma infiltration into the brain parenchyma is enhanced by overexpression of endogenous tenascin-C, which induces reactive changes of the brain tissues, detected as hyperintensity area with FLAIR sequences.

Discussion

Numerous studies have revealed that tenascin-C plays a certain role in tumor progression including tumorigenesis, proliferation, invasion, metastasis and angiogenesis.[14,15,18,19,22,32–38] It is widely acknowledged that tenascin-C disrupts the binding of fibronectin to the integrin $\alpha_5\beta_1$/syndecan-4 complex at the cell surface, which causes morphological change of cultured cells and promotes cell proliferation.[22,39,40] However, in this study, no significant differences exist in cell morphology or proliferation between the control and tenascin-C-knockdown glioblastoma cells. This is possibly because tenascin-C affects cell growth and morphology in an environment containing extrinsic tenascin-C and fibronectin.[20,33] While collagen, fibronectin and laminin are the predominant ECM components in non-central nervous system tissue, major ECM components of brain parenchyma include hyaluronan, proteoglycans and glycosaminoglycans, such as hyaluronic acid and chondroitin sulfate. Fibronectin is found at the gliomesenchymal junction of tumors and in tumor-associated blood vessels.[41] Glioblastomas do not express fibronectin, yet fibronectin is confined to proliferating vessel walls and leptomeninges.[42] Fibronectin was either localized in the basement membrane or formed thick, multi-layered deposits in the vessel walls. Fibronectin expression was seen in all glioblastoma samples but

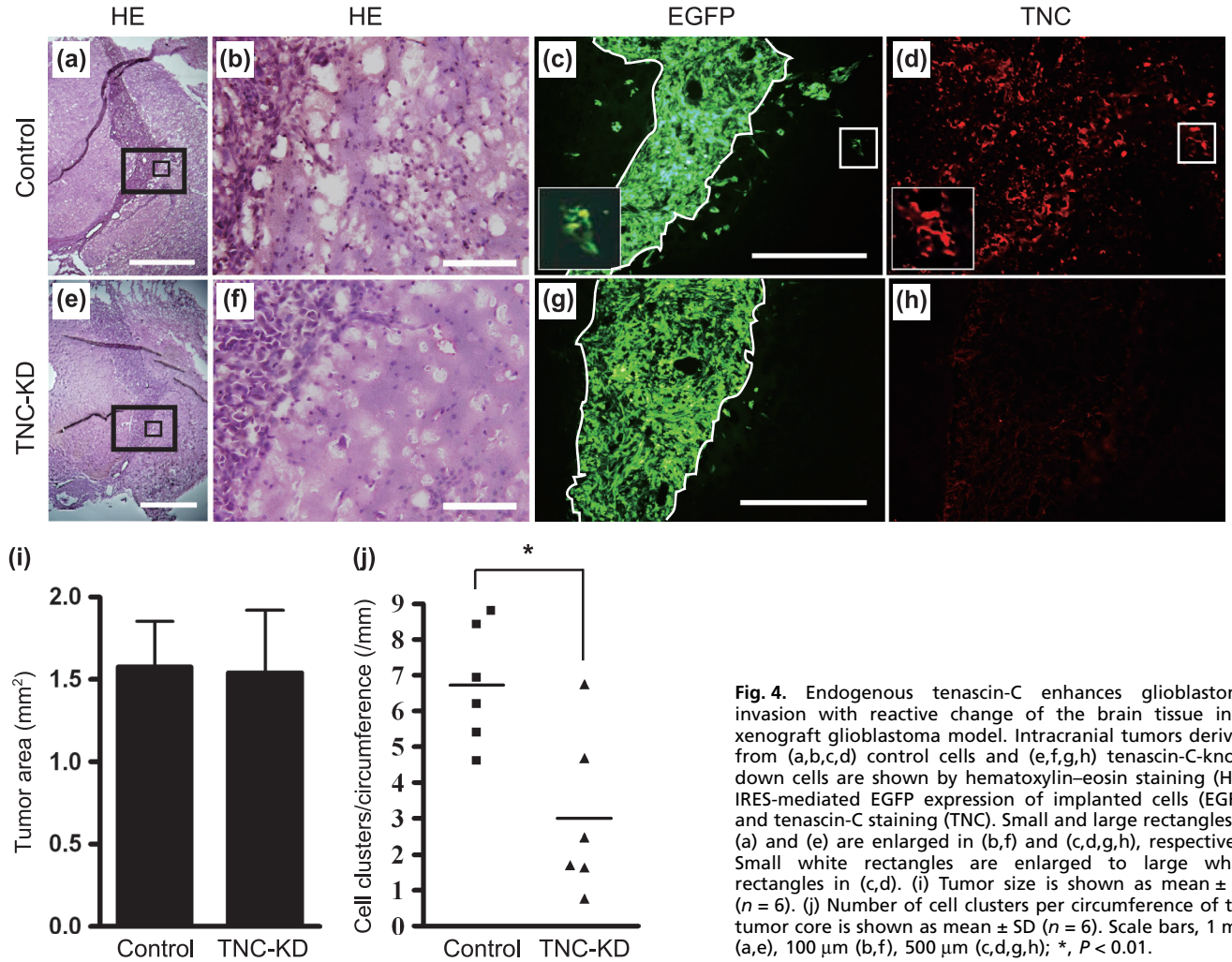

Fig. 4. Endogenous tenascin-C enhances glioblastoma invasion with reactive change of the brain tissue in a xenograft glioblastoma model. Intracranial tumors derived from (a,b,c,d) control cells and (e,f,g,h) tenascin-C-knock down cells are shown by hematoxylin–eosin staining (HE), IRES-mediated EGFP expression of implanted cells (EGFP) and tenascin-C staining (TNC). Small and large rectangles in (a) and (e) are enlarged in (b,f) and (c,d,g,h), respectively. Small white rectangles are enlarged to large white rectangles in (c,d). (i) Tumor size is shown as mean ± SD (n = 6). (j) Number of cell clusters per circumference of the tumor core is shown as mean ± SD (n = 6). Scale bars, 1 mm (a,e), 100 μm (b,f), 500 μm (c,d,g,h); *, $P < 0.01$.

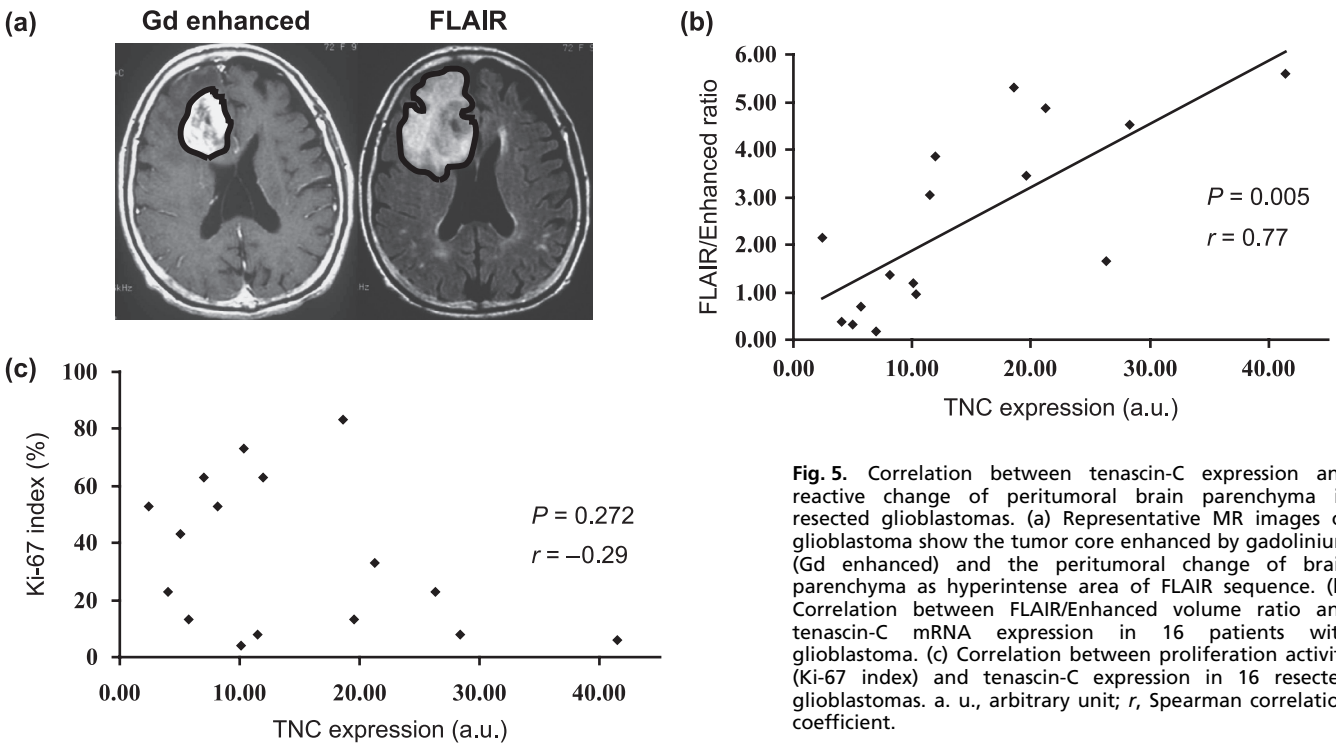

Fig. 5. Correlation between tenascin-C expression and reactive change of peritumoral brain parenchyma in resected glioblastomas. (a) Representative MR images of glioblastoma show the tumor core enhanced by gadolinium (Gd enhanced) and the peritumoral change of brain parenchyma as hyperintense area of FLAIR sequence. (b) Correlation between FLAIR/Enhanced volume ratio and tenascin-C mRNA expression in 16 patients with glioblastoma. (c) Correlation between proliferation activity (Ki-67 index) and tenascin-C expression in 16 resected glioblastomas. a. u., arbitrary unit; r, Spearman correlation coefficient.

doi: 10.1111/j.1349-7006.2009.01189.x

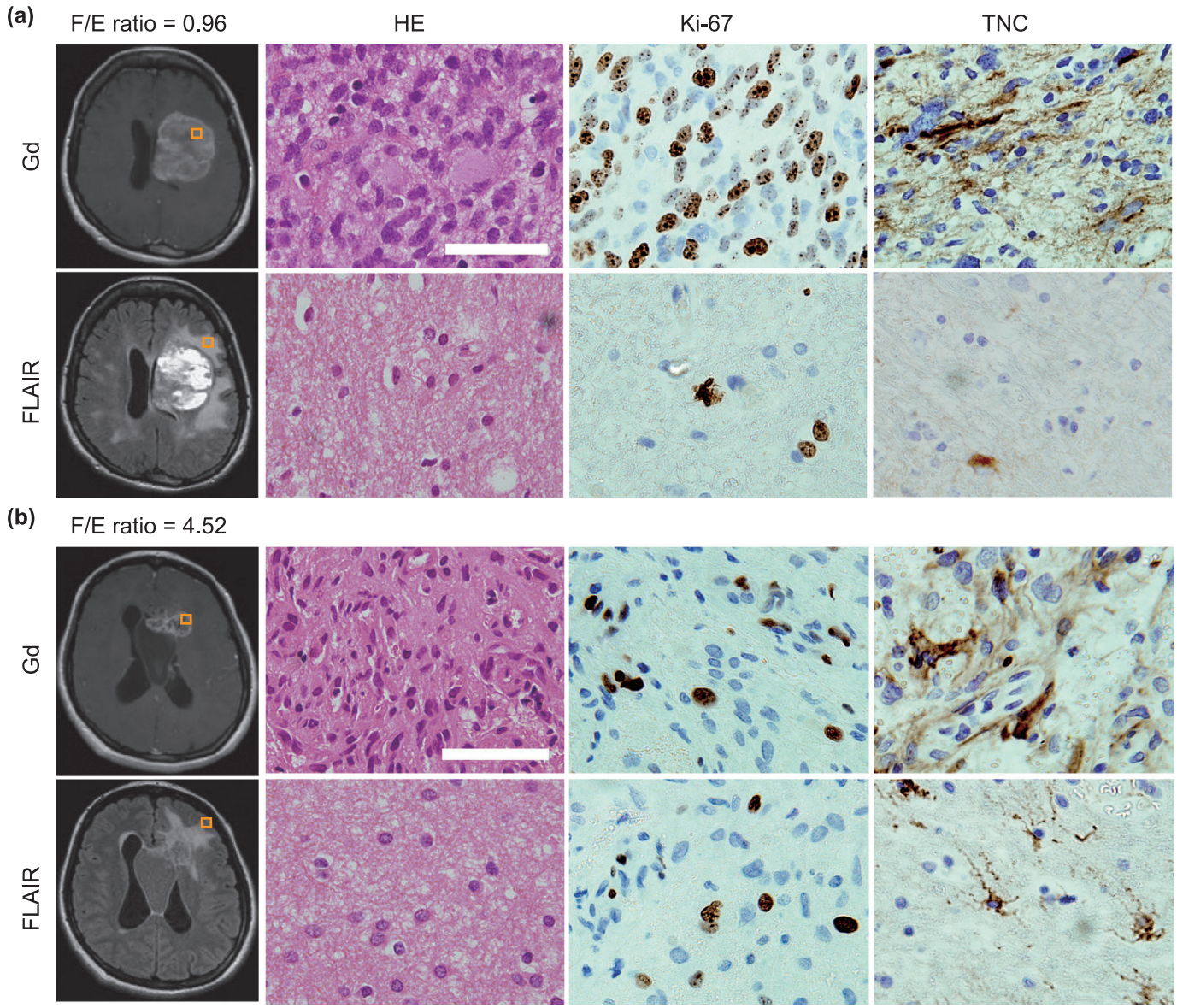

Fig. 6. Infiltrating glioblastoma cells show cytoplasmic deposition of tenascin-C in reactive changes of peritumoral brain parenchyma detected by FLAIR image. Representative images of the tumor core and peritumoral tissue in patients with (a) low FLAIR/Enhanced volume ratio (F/E ratio) and (b) high F/E ratio. Each square in MR images (left panel) indicates the localization of the microscopic images (three right panels; HE, Ki-67, TNC). Hematoxylin–eosin staining (HE), mitotic activity staining (Ki-67), tenascin-C staining (TNC). Scale bars, 200 μm.

its distribution was not uniform, and its staining intensity was weak.[31] These observations suggest that endogenous tenascin-C secreted by glioblastoma cells does not affect cell morphology and proliferation when the tumor microenvironment does not abound in fibronectin.

In this study, glioblastoma cell motility on a non-coated substrate was significantly suppressed in tenascin-C-knockdown cells, indicating that endogenous tenascin-C accelerates glioblastoma cell invasion via different machinery from the action of tenascin-C on fibronectin. The same phenotype was also seen in a xenograft model whereby tenascin-C-knockdown glioblastoma cells exhibited less invasiveness into brain parenchyma. Immunohistochemical localization of tenascin-C *in vivo* experiments and clinical samples demonstrate predominant cytoplasmic deposition in the glioblastoma cells invading into brain tissue, especially in the patient with high F/E ratio, which shows highly invasive tumor. These observations suggest that glioblastoma cells with abundant expression of tenascin-C invade aggressively and secreted tenascin-C acts to enhance their invasiveness in an autocrine manner. Tenascin-C was described as a hexabrachion because it exists as a hexamer of 220–320-kDa subunits. Each subunit of tenascin-C comprises three types of structural modules: EGF-like domains, fibronectin type III (FNIII) repeat domains, and a terminal knob homologous to the beta- and gamma-chains of fibrinogen. This multidomain structure of the tenascin-C suggests the possibility of multiple independent functions.[43] In this study, we confirmed that extrinsic tenascin-C rescued the migration disorder of tenascin-C knockdown cells. It is a possible mechanism that endogenous tenascin-C is involved in the regulation of focal adhesion turnover.

The expression level of tenascin-C correlates with prognosis in patients with many malignancies.[14,37,44–49] In the previous study, we identified tenascin-C expression as prognosis factor of patients with glioblastoma.[9] The invasive nature of gliomas also causes breakdown of the blood–brain barrier and cerebral edema formation, which is responsible for significant morbidity and

mortality in patients with glioblastoma. In this study, we found that the expression level of tenascin-C correlates with the degree of peritumoral change in brain parenchyma. This change in brain parenchyma is thought to be comprised of focal brain edema and changes of extracellular matrix following glioblastoma cell invasion; however, the underlying mechanism is still unclear.

The change of the peritumoral brain tissue is usually detected as hyperintensity in T2-weighted images and FLAIR sequences of MR imaging.[2,3,7] Regrettably, it was impossible to evaluate discriminatively the gadolinium-enhanced tumor core and the peritumoral hyperintensity area in our mouse xenograft model. In the immunohistochemical analysis, diffuse deposition of tenascin-C was observed in the stroma of the tumor core and peritumoral brain tissue. Interestingly, strong cytoplasmic deposition of tenascin-C was detected in the migrating glioblastoma cells at the invasion border and in the peritumoral brain tissue. In a study of breast cancer cells, Ishihara *et al*. emphasized that cancer spreading might be involved in cytoplasmic deposition of tenascin-C, but not in intercellular deposition.[50] Taken together, tenascin-C may be one of the key extracellular matrix components facilitating glioblastoma cell invasion and promoting the peritumoral change of brain parenchyma.

In summary, we report that endogenous tenascin-C facilitates glioblastoma cell invasion by regulating focal adhesion and that glioblastoma cells with high tenascin-C expression exhibit invasive nature. Consistent with these observations, the expression level of tenascin-C correlates with the degree of peritumoral tissue change, detected as FLAIR hyperintensity in clinical samples. The detail molecular basis for this curious ability of endogenous tenascin-C to facilitate glioblastoma cell invasion is still unclear and warrants further investigation. This study highlights tenascin-C's attractiveness as a target molecule for anti-invasion therapy in the treatment of glioblastoma.

Acknowledgments

We thank M Way (Cancer Research UK, London) for reagents. We thank members of Arakawa's and Matsuda's laboratories for constructive comments on the manuscript and throughout the project. This work was supported by grants from a Grant-in-Aid for Specially Promoted Research from the Ministry for Education, Culture, Sports, Science and Technology of Japan (YA, YK, JAT, MM, NH), Kyoto University Research Fund (YA) and Japan Heart Foundation/Bayer Yakuhin Research Grant (YA).

Disclosure Statement

We declare that we have no competing financial interests.

References

1 Kleihues P, Burger PC, Scheithauer BW. The new WHO classification of brain tumours. *Brain Pathol* 1993; **3**: 255–68.
2 Nakada M, Nakada S, Demuth T, Tran NL, Hoelzinger DB, Berens ME. Molecular targets of glioma invasion. *Cell Mol Life Sci* 2007; **64**: 458–78.
3 Henson JW, Gaviani P, Gonzalez RG. MRI in treatment of adult gliomas. *Lancet Oncol* 2005; **6**: 167–75.
4 Ishihara H, Kubota H, Lindberg RL *et al*. Endothelial cell barrier impairment induced by glioblastomas and transforming growth factor beta2 involves matrix metalloproteinases and tight junction proteins. *J Neuropathol Exp Neurol* 2008; **67**: 435–48.
5 McKeever PE, Varani J, Papadopoulos SM, Wang M, McCoy JP. Products of cells from gliomas: IX. Evidence that two fundamentally different mechanisms change extracellular matrix expression by gliomas. *J Neurooncol* 1995; **24**: 267–80.
6 Ganslandt O, Stadlbauer A, Fahlbusch R *et al*. Proton magnetic resonance spectroscopic imaging integrated into image-guided surgery: correlation to standard magnetic resonance imaging and tumor cell density. *Neurosurgery* 2005; **56**: 291–8.
7 Claes A, Idema AJ, Wesseling P. Diffuse glioma growth: a guerilla war. *Acta Neuropathol* 2007; **114**: 443–58.
8 Nutt CL, Mani DR, Betensky RA *et al*. Gene expression-based classification of malignant gliomas correlates better with survival than histological classification. *Cancer Res* 2003; **63**: 1602–7.
9 Shirahata M, Iwao-Koizumi K, Saito S *et al*. Gene expression-based molecular diagnostic system for malignant gliomas is superior to histological diagnosis. *Clin Cancer Res* 2007; **13**: 7341–56.
10 Demuth T, Berens ME. Molecular mechanisms of glioma cell migration and invasion. *J Neurooncol* 2004; **70**: 217–28.
11 Furnari FB, Fenton T, Bachoo RM *et al*. Malignant astrocytic glioma: genetics, biology, and paths to treatment. *Genes Dev* 2007; **21**: 2683–710.
12 Yamana N, Arakawa Y, Nishino T *et al*. The Rho-mDia1 pathway regulates cell polarity and focal adhesion turnover in migrating cells through mobilizing Apc and c-Src. *Mol Cell Biol* 2006; **26**: 6844–58.
13 Katz BZ, Romer L, Miyamoto S *et al*. Targeting membrane-localized focal adhesion kinase to focal adhesions: roles of tyrosine phosphorylation and SRC family kinases. *J Biol Chem* 2003; **278**: 29115–20.
14 Orend G, Chiquet-Ehrismann R. Tenascin-C induced signaling in cancer. *Cancer Lett* 2006; **244**: 143–63.
15 Chiquet-Ehrismann R. Tenascins. *Int J Biochem Cell Biol* 2004; **36**: 986–90.
16 Kawakatsu H, Shiurba R, Obara M, Hiraiwa H, Kusakabe M, Sakakura T. Human carcinoma cells synthesize and secrete tenascin in vitro. *Jpn J Cancer Res* 1992; **83**: 1073–80.
17 Sugawara I, Hirakoshi J, Kusakabe M, Masunaga A, Itoyama S, Sakakura T. Relationships among tenascin expression, DNA ploidy patterns, and multidrug resistance gene product (P-glycoprotein) in human colon carcinoma. *Jpn J Cancer Res* 1993; **84**: 703–7.
18 Sarkar S, Nuttall RK, Liu S, Edwards DR, Yong VW. Tenascin-C stimulates glioma cell invasion through matrix metalloproteinase-12. *Cancer Res* 2006; **66**: 11771–80.
19 Zagzag D, Shiff B, Jallo GI *et al*. Tenascin-C promotes microvascular cell migration and phosphorylation of focal adhesion kinase. *Cancer Res* 2002; **62**: 2660–8.
20 Ruiz C, Huang W, Hegi ME *et al*. Growth promoting signaling by tenascin-C [corrected]. *Cancer Res* 2004; **64**: 7377–85.
21 Deryugina EI, Bourdon MA. Tenascin mediates human glioma cell migration and modulates cell migration on fibronectin. *J Cell Sci* 1996; **109** (Pt 3): 643–52.
22 Lange K, Kammerer M, Hegi ME *et al*. Endothelin receptor type B counteracts tenascin-C-induced endothelin receptor type A-dependent focal adhesion and actin stress fiber disorganization. *Cancer Res* 2007; **67**: 6163–73.
23 Matsumoto K, Takahashi K, Yoshiki A, Kusakabe M, Ariga H. Invasion of melanoma in double knockout mice lacking tenascin-X and tenascin-C. *Jpn J Cancer Res* 2002; **93**: 968–75.
24 Rubinson DA, Dillon CP, Kwiatkowski AV *et al*. A lentivirus-based system to functionally silence genes in primary mammalian cells, stem cells and transgenic mice by RNA interference. *Nat Genet* 2003; **33**: 401–6.
25 Arakawa Y, Cordeiro JV, Schleich S, Newsome TP, Way M. The release of vaccinia virus from infected cells requires RhoA-mDia modulation of cortical actin. *Cell Host Microbe* 2007; **1**: 227–40.
26 Candolfi M, Curtin JF, Nichols WS *et al*. Intracranial glioblastoma models in preclinical neuro-oncology: neuropathological characterization and tumor progression. *J Neurooncol* 2007; **85**: 133–48.
27 Toda Y, Kono K, Abiru H *et al*. Application of tyramide signal amplification system to immunohistochemistry: a potent method to localize antigens that are not detectable by ordinary method. *Pathol Int* 1999; **49**: 479–83.
28 Oda M, Arakawa Y, Kano H *et al*. Quantitative analysis of topoisomerase IIalpha to rapidly evaluate cell proliferation in brain tumors. *Biochem Biophys Res Commun* 2005; **331**: 971–6.
29 Chiquet-Ehrismann R, Chiquet M. Tenascins: regulation and putative functions during pathological stress. *J Pathol* 2003; **200**: 488–99.
30 Midwood KS, Schwarzbauer JE. Tenascin-C modulates matrix contraction via focal adhesion kinase- and Rho-mediated signaling pathways. *Mol Biol Cell* 2002; **13**: 3601–13.
31 Oz B, Karayel FA, Gazio NL, Ozlen F, Balci K. The distribution of extracellular matrix proteins and CD44S expression in human astrocytomas. *Pathol Oncol Res* 2000; **6**: 118–24.
32 Behrem S, Zarkovic K, Eskinja N, Jonjic N. Distribution pattern of tenascin-C in glioblastoma: correlation with angiogenesis and tumor cell proliferation. *Pathol Oncol Res* 2005; **11**: 229–35.
33 Huang W, Chiquet-Ehrismann R, Moyano JV, Garcia-Pardo A, Orend G. Interference of tenascin-C with syndecan-4 binding to fibronectin blocks cell adhesion and stimulates tumor cell proliferation. *Cancer Res* 2001; **61**: 8586–94.
34 Mahesparan R, Read TA, Lund-Johansen M, Skaftnesmo KO, Bjerkvig R,

doi: 10.1111/j.1349-7006.2009.01189.x

Engebraaten O. Expression of extracellular matrix components in a highly infiltrative in vivo glioma model. *Acta Neuropathol* 2003; **105**: 49–57.
35 Zagzag D, Friedlander DR, Dosik J *et al*. Tenascin-C expression by angiogenic vessels in human astrocytomas and by human brain endothelial cells in vitro. *Cancer Res* 1996; **56**: 182–9.
36 Zagzag D, Friedlander DR, Miller DC *et al*. Tenascin expression in astrocytomas correlates with angiogenesis. *Cancer Res* 1995; **55**: 907–14.
37 Herold-Mende C, Mueller MM, Bonsanto MM, Schmitt HP, Kunze S, Steiner HH. Clinical impact and functional aspects of tenascin-C expression during glioma progression. *Int J Cancer* 2002; **98**: 362–9.
38 Giuffrida A, Scarpa S, Birarelli P, Modesti A. The interaction of tenascin-C with fibronectin modulates the migration and specific metalloprotease activity in human mesothelioma cell lines of different histotype. *Int J Oncol* 2004; **25**: 745–50.
39 Wenk MB, Midwood KS, Schwarzbauer JE, Tenascin C suppresses Rho activation. *J Cell Biol* 2000; **150**: 913–20.
40 Midwood KS, Valenick LV, Hsia HC, Schwarzbauer JE. Coregulation of fibronectin signaling and matrix contraction by tenascin-C and syndecan-4. *Mol Biol Cell* 2004; **15**: 5670–7.
41 Chintala SK, Sawaya R, Gokaslan ZL, Fuller G, Rao JS. Immunohistochemical localization of extracellular matrix proteins in human glioma, both in vivo and in vitro. *Cancer Lett* 1996; **101**: 107–14.
42 Kochi N, Tani E, Morimura T, Itagaki T. Immunohistochemical study of fibronectin in human glioma and meningioma. *Acta Neuropathol* 1983; **59**: 119–26.
43 Erickson HP, Bourdon MA. Tenascin: an extracellular matrix protein prominent in specialized embryonic tissues and tumors. *Annu Rev Cell Biol* 1989; **5**: 71–92.
44 Brunner A, Mayerl C, Tzankov A *et al*. Prognostic significance of tenascin-C expression in superficial and invasive bladder cancer. *J Clin Pathol* 2004; **57**: 927–31.
45 Dandachi N, Hauser-Kronberger C, More E *et al*. Co-expression of tenascin-C and vimentin in human breast cancer cells indicates phenotypic transdifferentiation during tumour progression: correlation with histopathological parameters, hormone receptors, and oncoproteins. *J Pathol* 2001; **193**: 181–9.
46 Gulubova MV, Vlaykova TI. Significance of tenascin-C, fibronectin, laminin, collagen IV, alpha5beta1 and alpha9beta1 integrins and fibrotic capsule formation around liver metastases originating from cancers of the digestive tract. *Neoplasma* 2006; **53**: 372–83.
47 Ilmonen S, Jahkola T, Turunen JP, Muhonen T, Asko-Seljavaara S. Tenascin-C in primary malignant melanoma of the skin. *Histopathology* 2004; **45**: 405–11.
48 Leins A, Riva P, Lindstedt R, Davidoff MS, Mehraein P, Weis S. Expression of tenascin-C in various human brain tumors and its relevance for survival in patients with astrocytoma. *Cancer* 2003; **98**: 2430–9.
49 Salmenkivi K, Haglund C, Arola J, Heikkila P. Increased expression of tenascin in pheochromocytomas correlates with malignancy. *Am J Surg Pathol* 2001; **25**: 1419–23.
50 Ishihara A, Yoshida T, Tamaki H, Sakakura T. Tenascin expression in cancer cells and stroma of human breast cancer and its prognostic significance. *Clin Cancer Res* 1995; **1**: 1035–41.